AGU PUBLICATIONS

Water Resources Research

RESEARCH ARTICLE
10.1002/2015WR017154

Rapid identification of transience in streambed conductance by inversion of floodwave responses

Guillaume Gianni[1], Julien Richon[2], Pierre Perrochet[1], Alexandre Vogel[3], and Philip Brunner[1]

[1]Center for Hydrogeology and Geothermics, University of Neuchâtel, Switzerland, [2]Bureau d'Études Géologiques SA, Aproz, Switzerland, [3]Rhône River Flood Protection Services, Canton of Valais, Switzerland

Key Points:
- Method assessing transience in streambed conductance
- Application of the method to synthetic and field data
- The transience in streambed is related to stream dynamics

Correspondence to:
G. Gianni,
guillaume.gianni@unine.ch

Citation:
Gianni, G., J. Richon, P. Perrochet, A. Vogel, and P. Brunner (2016), Rapid identification of transience in streambed conductance by inversion of floodwave responses, *Water Resour. Res.*, *52*, 2647–2658, doi:10.1002/2015WR017154.

Received 3 MAR 2015
Accepted 1 FEB 2016
Accepted article online 5 FEB 2016
Published online 6 APR 2016

Abstract Streambed conductance controls the interaction between surface and groundwater. However, the streambed conductance is often subject to transience. Directly measuring hydraulic properties in a river yields only point values, is time-consuming and therefore not suited to detect transience of physical properties. Here, we present a method to continuously monitor transience in streambed conductance. Input data are time series of stream stage and near stream hydraulic head. The method is based on the inversion of floodwave responses. The analytical model consists of three parameters: x, the distance between streambank and an observation well, α, the aquifer diffusivity, and a the retardation coefficient that is inversely proportional to the streambed conductance. Estimation of a is carried out over successive time steps in order to identify transience in streambed conductance. The method is tested using synthetic data and is applied to field data from the Rhône River and its alluvial aquifer (Switzerland). The synthetic method demonstrated the robustness of the proposed methodology. Application of the method to the field data allowed identifying transience in streambed properties, following flood events in the Rhône. This method requires transience in the surface water, and the river should not change its width significantly with a rising water level. If these conditions are fulfilled, this method allows for a rapid and effective identification of transience in streambed conductance.

1. Introduction

River-aquifer exchanges have been the focus of much research, due to its importance in water quality and quantity management, e.g., river bank filtration systems [*Hiscock and Grischek*, 2002], river restorations [*Kurth and Schirmer,* 2014], or contaminant transport across the interface of surface water and groundwater [*Smith and Lerner,* 2008]. One of the key factors that controls river-groundwater interactions is the streambed [*Sophocleous,* 2002; *Winter et al.*, 1998]. The streambed composition is continuously affected by sedimentation and erosion [*Coleman*, 1969; *Levy et al.*, 2011; *Schalchli*, 1992], chemical [*Du et al.*, 2013; *Smith and Lerner*, 2008] and biological processes [*Wang et al.*, 2014]. These changes affect the hydraulic properties of the streambed and cause variations in streambed hydraulic properties, such as its hydraulic conductivity and heterogeneity [*Irvine et al.*, 2012; *Kalbus et al.*, 2009; *Levy et al.*, 2011; *Simpson and Meixner*, 2012].

Changes of up to two orders of magnitude of the streambed hydraulic conductivity after flood events have been documented in field studies [*Fette et al.*, 2005; *Genereux et al.*, 2008; *Hatch et al.*, 2010; *Wu et al.*, 2015]. Such changes significantly affect the exchange fluxes between the surface and the groundwater domains. If this transience is not taken into account, predictions on exchange fluxes will be unreliable. For example, numerical models simulating the interactions between surface water and groundwater typically assume streambed conductance to be constant. If streambed properties are transient, however, this assumption will cause a systematic bias to model predictions. It is therefore critical to understand if the system modelled is subject to such transience.

Several approaches to measure streambed hydraulic conductivity are commonly used, e.g., seepage meters [*Rosenberry,* 2008; *Woessner and Sullivan,* 1984], permeameters [*Landon et al.*, 2001; *Lee et al.*, 2015], laboratory measurements of streambed samples [*Rosenberry and Pitlick*, 2009; *Schalchli*, 1992], thermal methods [*Hatch et al.*, 2010; *Mutiti and Levy*, 2010]. More recently, reach scale evaluation of the streambed hydraulic conductivity based on streamflow-front velocities has been proposed by *Shanafield et al.* [2014]. However, all of these methods are time consuming. Also, the high degree of heterogeneity typically found in

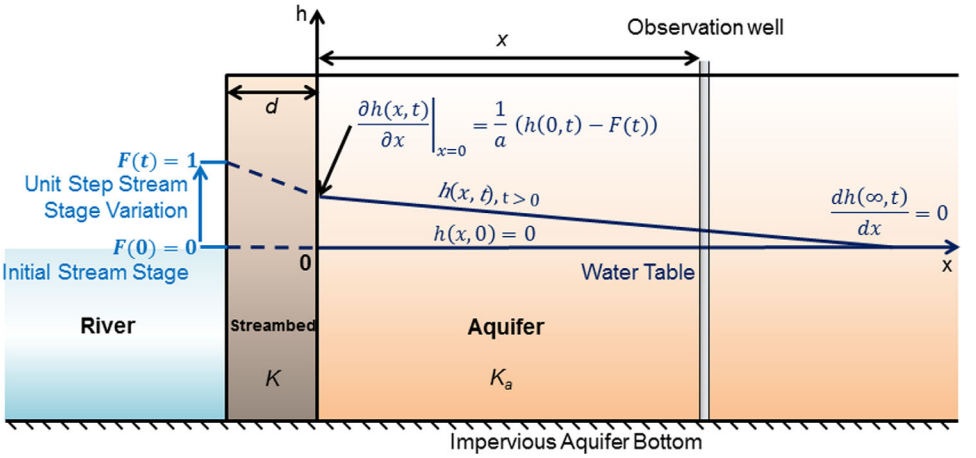

Figure 1. Sketch of the mathematical model describing the propagation of head $h(x,t)$ that represents the aquifer response to a unit step increase of the stream stage along with the initial and boundary conditions (2)–(4). K_a is the aquifer hydraulic conductivity, K is the streambed hydraulic conductivity, d is the streambed thickness, and x is the distance between the streambed and the observation well. The stream is considered fully penetrating and is separated from the aquifer by a homogeneous vertical layer.

streambeds [*Calver*, 2001] makes point measurements of hydraulic properties difficult. Given the difficulty of directly measuring hydraulic properties of a streambed, detecting transience in these properties is even more challenging.

We present a method, requiring only stream stage and near stream water table time series, that under given conditions allows identifying transience in streambed hydraulic properties (specifically streambed conductance). The method is based on a succession of inversion of an analytical model [*Ha et al.*, 2007; *Jha and Singh*, 2014; *Jha et al.*, 2008; *Reynolds*, 1987], i.e., a floodwave response model [*Hall and Moench*, 1972; *Jha et al.*, 2004]. This analytical model calculates the aquifer response, in terms of hydraulic head, as a function of stream stage variations. The approach allows estimating the retardation coefficient [*Hall and Moench*, 1972; *Hantush*, 1965], which is inversely proportional to the streambed conductance. We show that estimating this parameter for successive time steps allows detecting changes in the streambed conductance. This approach is tested using synthetic data and field measurements from the Rhône River and its alluvial aquifer (Switzerland).

2. Methods

2.1. Overview

The presented method is based on the response of an aquifer to transience in the river stage. The required input data and parameters are: continuous stream stage and riparian water table time series, distance of the observation well to the streambank as well as the diffusivity of the aquifer. The method consists of three iterative steps: (1) the floodwave response is calculated using a convolution between an aquifer unit step response and stream stage variations; (2) the discrepancies between simulated aquifer responses and field observations are minimized by estimation of the retardation coefficient; (3) this inversion is repeated for successive time steps in order to detect variations in the estimated retardation coefficient and thus in the streambed conductance.

2.2. Floodwave Response Model

The variation of hydraulic head h [L] in one dimension in terms of distance x [L], and time t [T] can be expressed through equation (1):

$$\frac{\partial h(x,t)}{\partial t} = \alpha \frac{\partial^2 h(x,t)}{\partial x^2} \tag{1}$$

where α [$L^2\ T^{-1}$] is the hydraulic diffusivity, expressed by the ratio $K_a d_a/S$ where K_a [$L\ T^{-1}$] is the hydraulic conductivity of the aquifer, d_a [L] the thickness of the aquifer, and S is the storativity. Figure 1 illustrates the

conceptual model used to develop and solve equation (1) in order to calculate the aquifer response to variations of stream stage. This requires an initial condition (equation (2)) and boundary conditions (equations (3) and (4)). These equations represent the hydraulic head variations of an aquifer of infinite horizontal extent to a step variation of the stream stage. It is assumed that the initial hydraulic head throughout the aquifer and of the stream stage is equal to 0, and that a streambed with hydraulic properties different to the aquifer is present:

$$h(x,0)=0 \tag{2}$$

$$dh/dx(\infty,t)=0 \tag{3}$$

$$\left.\frac{\partial h(x,t)}{\partial x}\right|_{x=0}=\frac{1}{a}\left(h(0,t)-F(t)\right) \tag{3}$$

where $F(t)$ [L] represents the stream stage and is equal to 1 after a unit step variation. a [L] is the retardation coefficient and represents the effective thickness of aquifer required to cause the same head loss as the streambed layer [*Hantush*, 1965]. a is expressed by dK_a/K, where d [L] is the thickness of the streambed and K [L T^{-1}] the hydraulic conductivity of the streambed. The retardation coefficient is inversely proportional to the streambed conductance per square meter C [T^{-1}], defined as K/d [*Hantush*, 1965; *Kollet and Zlotnik*, 2007]. The distance x represents the distance from the streambank. The analytical solution of equation (1) along with equations (2)–(4) is given by [*Carslaw and Jaeger*, 1959; *Hall and Moench*, 1972]:

$$h(x,t)=\operatorname{erfc}\left(\frac{x}{2\sqrt{\alpha t}}\right)-\exp\left(\frac{x}{a}+\frac{\alpha t}{a^2}\right)\operatorname{erfc}\left(\frac{x}{2\sqrt{\alpha t}}+\frac{\sqrt{\alpha t}}{a}\right) \tag{5}$$

where erfc and exp are the complementary error function and the exponential function. The variable x represents the distance from the outer edge of the streambank along the x axis. In practice, x represents the distance to the streambank of a vertical observation well from which water table time series are recorded.

Only three parameters are used in equation (5): the distance between the observation well and the streambank x, the diffusivity of the aquifer α, and the retardation coefficient a. The first term on the right hand side of equation (5) represents the aquifer response without a clogging layer. The second term represents the effect of the streambed on the aquifer response. Increase in the value of a will increase the head loss generated by the streambed.

Using the analytical solution (equation (5)), referred from now on as $P(x,t)$, *Hall and Moench* [1972] presented a convolution method to solve aquifer response to any stream stage variation. Assuming $F(0)=0$, the hydraulic head $h(x,t)$ is calculated using the convolution product:

$$h(x,t)=\int_0^t F'(\tau)\ P(x,t-\tau)\ d\tau \tag{6}$$

where $F'(t)$ is the stream stage variation and τ is the variable of integration. The discrete form of equation (6) is the following:

$$h(x,n\Delta t)=\sum_{k=1}^{n-1}\int_{k\Delta t}^{(k+1)\Delta t} F'(u)\ P(x,\ n\Delta t-u)\ du \tag{7}$$

where n is the number of discrete time steps of constant length Δt, k is the index of summation, and u is the variable of integration. Assuming a linear variation of the function between two successive time steps, equation (7) becomes:

$$h(x,n\Delta t)=\sum_{k=1}^{n-1}\frac{\Delta t}{6}\left(F'_kP_{n-k}+F'_{k+1}P_{n-k+1}+2F'_kP_{n-k+1}+2F'_{k+1}P_{n-k}\right) \tag{8}$$

Equation (8) will be used from here on to numerically compute the aquifer response to stream stage variations. The influence of the numerous simplifying assumptions on the applicability and reliability of the proposed method to identify streambed conductance transience will be discussed in section 5.

2.3. Retardation Coefficients Estimation

The retardation coefficient a can be estimated using parameter estimation approaches which minimize the Sum of Squared Error (SSE) between observed and calculated heads:

$$SSE = \sum_{i=1}^{m} (H_i - h_i)^2 \tag{9}$$

where m is the number of hydraulic head field observations H, within a given time interval, and h_i its calculated counterpart at time i. We used a gradient descent algorithm based on the variation of equation (9) with a termination criterion consisting of a minimum residual of estimated a between two time steps. Other parameter estimation approaches could also be used (e.g., a Monte-Carlo approach).

In order to detect transience in the retardation coefficient, the available time series of field data are subdivided in successive and partially overlapping time intervals, referred to as Parameter Optimization Window (POW). Figure 2 illustrates the two parameters of the POW: the size [T] and the shift [T]. Within each POW, the retardation coefficient a is assumed to be constant and is estimated using stream stages and hydraulic heads time series contained in the POW. Therefore, the size of the POW determines the number of observations used during each inversion and the shift determines the total number of inversions and thus the number of estimations of the parameter a within the study period. The sensitivity of the estimation to the POW size has been explored and is presented in the next sections. The entire approach, including the convolution and the parameter estimation, was implemented in *MATLAB* [2014].

3. Synthetic Data Analysis and Sensitivity to the POW

3.1. Model Setup

Using numerical modeling we test (1) if the method proposed can detect transience in the streambed conductance and (2) the sensitivity of the results to the POW size. First, synthetic data are generated using the numerical simulator *HydroGeoSphere* [2013]. During the simulation, the streambed conductance is varied by changing the hydraulic conductivity of the streambed in time, and the groundwater responses to stream stage variations are calculated. Then the retardation coefficient a is estimated using the simulated observation data. Finally, the estimated and simulated streambed conductances are compared.

The model geometry is similar to the mathematical model in Figure 1, but of limited horizontal extent (500m wide). The depth of the cross section is 50 m. The initial condition is a hydrostatic head of 52 m throughout the entire model domain. The head condition imposed on the left side (stream side) starts with a value of 52 m (initial condition) and varies between 51 and 53 m in order to represent stream stage

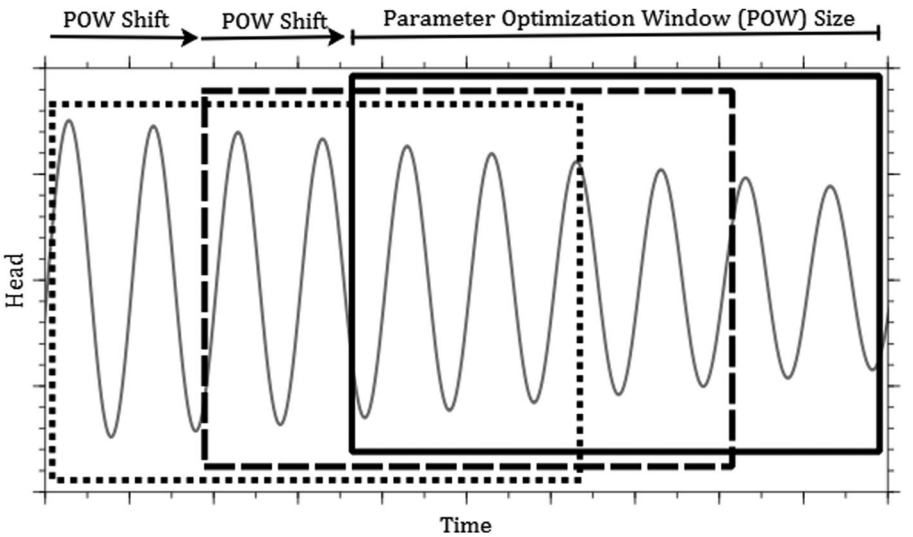

Figure 2. Parameter Optimization Window (POW) parameters: Size and Shift. Within each POW, the estimated retardation coefficient a is assumed constant and the inversion process estimates its value by minimizing the *SSE* between field and simulated hydraulic heads.

dynamics. The variations are generated using a sinusoidal function with a period of 1 day and a magnitude of 1 m (Figure 3b). On the opposite side (right side at 500 m from the stream side), a constant head boundary of 52 m is employed throughout the entire simulation. The bottom and top sides of the model are no flow boundaries. The aquifer has a homogeneous hydraulic conductivity K_a, of 1 md^{-1} and a specific storage S_s of 10^{-4} m^{-1}, the porous media is fully saturated and confined. The vertical streambed thickness, d, is 1 m. In order to represent clogging and unclogging processes, the streambed conductance C varies exponentially from 0.1 to 0.001 d^{-1} over 30 days. At the end of the 30th day, C is steeply raised from 0.001 to 0.1 d^{-1} within 0.01 days (around 15 min), simulating a fast unclogging of the streambed (e.g., erosion by a flood event or excavation in the streambed). Then the same exponential decrease is repeated a second time over another period of 30 days. Figure 3a shows the imposed C over the 60 days. The time series of stream stages variations and hydraulic heads generated by the simulation form the input data and calibration data of presented estimation process. The method is tested for different POW sizes: 1 day; 5 days; 10 days. The POW shift is 1 h. A residual value between two successive estimations of a of 0.1 m is used as termination criterion.

3.2. Results of the Synthetic Data Analysis

Figure 4 shows the imposed and estimated values of the retardation coefficient. The retardation coefficient a is estimated and the corresponding C value is calculated according to the known K_a value. In the same way, values of a are calculated in the forward simulation and then compared to the estimated values. On Figures 4b, 4c and 4d, the ratio of estimated C to imposed C is represented in order to monitor the accuracy of the estimation process.

Continuous variations of the streambed conductance are detected for the different POWS (Figures 4b–4d). Note that due to the size of the POW, the estimation of a was carried out between the 3rd and 57th day, and between the 5th and the 55th day for the POW sizes of 5 and 10 days, respectively.

For the three POW sizes, the value of a between the 1st and the 25th day are well estimated (i.e., between 50% and 150% of the impose values). The same is true for the timespan between the 35th and the 55th day. Between the 25th and 35th day, the accuracy of the estimation of a differs for the different POW sizes. During this period we observed that for increasing POW sizes the number of poorly matched values of a increases (i.e., under 50% or over 150% of the imposed conductance) increases. The bias in the estimation

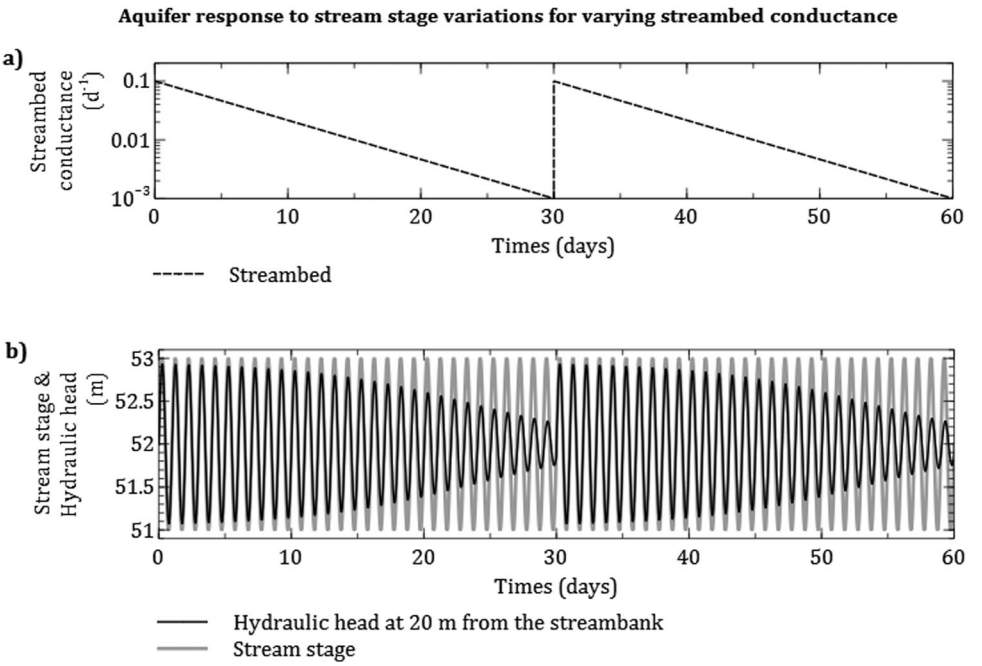

Figure 3. (a) Transience in streambed conductance. (b) The stream stage input function (sinusoid of period 1 day, magnitude 1 m, and damping factor of 0) and the groundwater response at 20 m from the streambank. The relation between the magnitude of the aquifer response and the value of the streambed conductance is clearly observed.

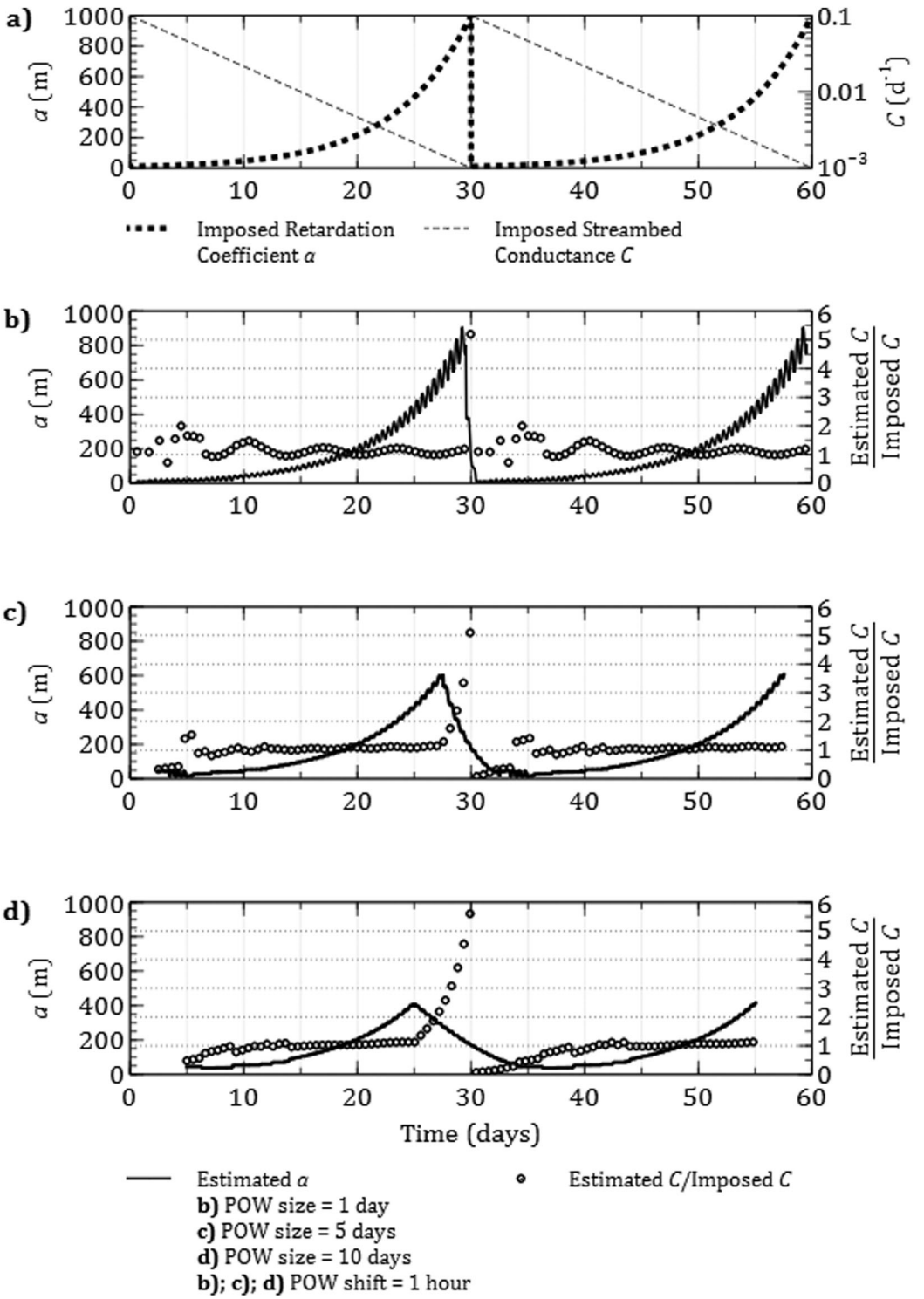

Figure 4. (a) Streambed conductance *C* imposed in the simulation and the corresponding retardation coefficient *a*. (b), (c), and (d) show the estimated retardation coefficient and the ratio of Estimated *C* to Imposed *C* for different values of the size of the Parameter Optimization Window (POW) (1, 5, and 10 days). The shift of the POW is 1 day for the three POW sizes. From Figures 4b–4d, a variation in the accuracy of the estimation of *a* with respect to the POW size can be observed.

of *a* appears when the POW includes hydraulic heads from before or after the sharp change of the imposed *C* on the 30th day. The highest error is made when the POW is centered on the sharp decrease of *C* (500% of the imposed *C*). Moreover, the beginning of the decrease appears 5 days and 10 days too early for the

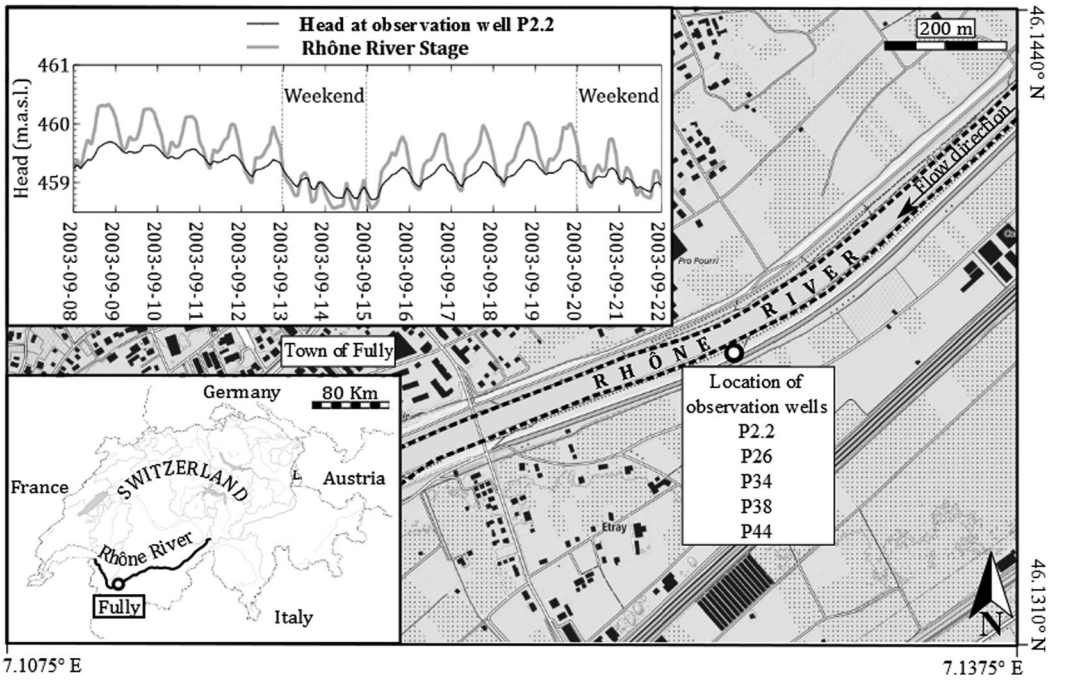

Figure 5. Map displaying the location of the study site, Town of Fully, and of the observation wells (WGS 84 coordinate system). The observation wells P2.2, P26, P34, P38, and P44 are located at 2.2, 26, 34, 38, and 44 m from the streambank. The graph (up left corner) shows the Rhône River variations and hydraulic heads at P2.2 during the month of September 2003. The daily variations of the Rhône River stage are due to the exploitation of hydroelectricity (lower stream stage during the weekend is due to lower electricity demand). Image source of the background map: Swiss Geoportal.

POW sizes of 5 and 10 days, respectively. It appears that the estimation of the value of a and its transience is increasingly biased when C undergoes a sharp and sudden alteration, for an increasing size of the POW.

In Figure 4b, sinusoidal variations of a are observed. These oscillations show that the parameter a tends to be systematically under-or overestimated. The reason for that is the sinusoidal variation of the stream stage and the fact that the convolution assumes an initially relaxed state of the system. A transient hydraulic head due to stream stage variation prior the current POW leads to an under-or overestimation of a. For larger POW sizes, this effect is reduced by the increasing ratio of water table variations triggered by stream transience in the current POW to water table variations triggered by stream transience in the previous POW. This analysis shows that the choice of POW can influence the estimated conductance. However, transience in streambed conductance was clearly identified, independent of the choice of the POW. As this method is aiming to identify whether streambed properties are subject to transience, a mismatch for the absolute value is not of concern.

4. Field Data Investigation

4.1. Study Site Description

The study site is a floodplain of the Rhône River located in the southern part of Switzerland (Figure 5). The Rhône glacial valley is filled with approximately 600 m of quaternary deposits [*Besson et al.*, 1991]. The lower 450 m are composed of a succession of different glacial deposits. A layer of fine lacustrine deposits is found from a depth between 150 to 50 m. This layer is considered as the lower limit of the alluvial aquifer. The 50 m thick alluvial aquifer is composed of post lacustrine gravelly river deposits. The aquifer is heterogeneous and composed by alternation of gravel and sandy silty-loam layers. The Rhône River is characterized by a glacionival dynamics with a high water level in summer and a low water level in winter. Daily variations of approximately 1 m of the Rhône River are caused by hydropeaking resulting from upstream hydroelectricity generation (Figure 5).

A river gauge and five observation wells are installed along a line perpendicular to the riverbank, P2.2, P26, P34, P38, and P44 with the respective distances from the river bank of 2.2, 26, 34, 38, and 44 m. The depth of measurement of each observation is approximately 5 m below the yearly average of the water table elevation at these points. The river is 52 m wide. The aquifer hydraulic conductivity and specific yield S_y was measured

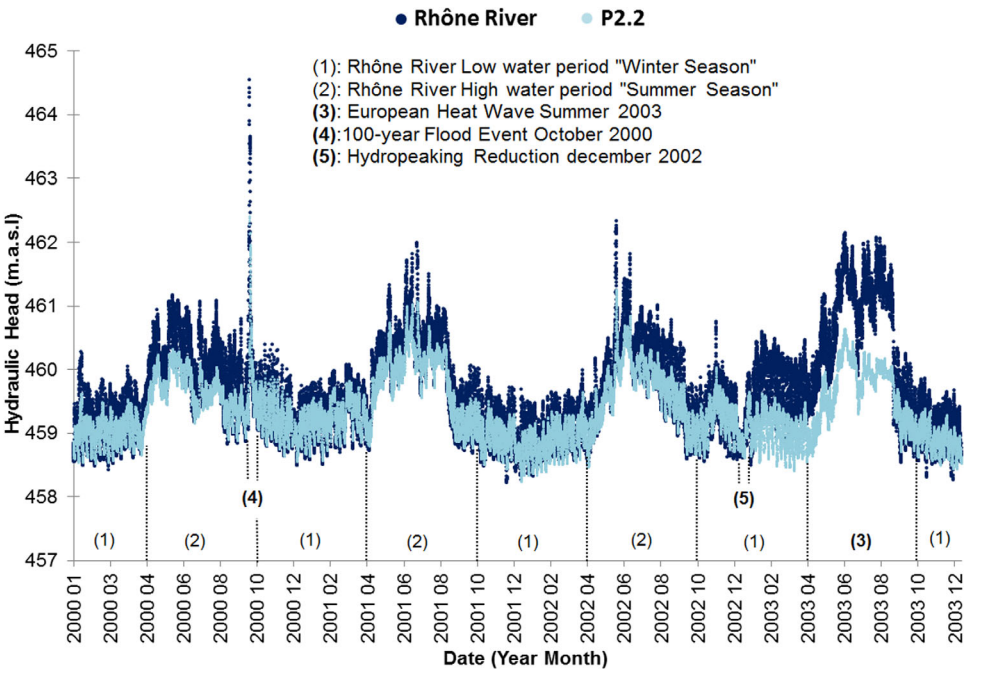

Figure 6. Rhône River (Fully, Switzerland) stage variations (dark blue dots) between 1 January 2000 and 31 December 2003, and the hydraulic head variations, during the same period, 2.2 m from the streambank (light blue dots). The estimation of the retardation coefficient a using this time series is shown in Figure 7. The time series is subdivided in five periods, with periods (1) and (2) that are repeated annually (low water period in winter and high water period in summer) and covers noteworthy events: a heat wave (3), a 100 year flood (4), and hydropeaking reduction (5).

through an aquifer test ($K_a = 6 \times 10^{-4}$ ms^{-1} and $S_y = 0.2$). The studied aquifer is unconfined, thus the storativity S, is approximated by the specific yield S_y, and an average-saturated thickness d_a of 50 m is used. A diffusivity of 0.15 m^{2}s^{-1} is calculated for this reach of the Rhône alluvial aquifer. The hydraulic head and stream stage data have been measured from 1 January 2000 to 31 December 2003 with a time step of 1 h. This timespan includes a 100 year flood event that happened on the 15 October 2000 Figure 6 shows the variations of the Rhône River stage (dark blue dots) and the variations of the water table at P2.2 (light blue dots).

4.2. Results

The retardation coefficient a is optimized for every POW shift of 1 day in order to fit the observed groundwater responses. The analysis is carried out for all boreholes individually. According to the daily periodic variations of the Rhône River in the study area due to hydropeaking (five significant variations of the stream stage a week), a POW size of 7 days covering a week of daily stream stage and hydraulic head transience was chosen. With this setting, we obtained a total number of POW of 1445 for each observation well. A residual value between two successive estimations of a of 0.1 m is used as a termination criteria for the parameter estimation. Figure 6 shows the time series data of the stream stage and the observation well P2.2 (for the sake of clarity the other boreholes are not plotted). In order to quantify how well the simplified analytical solution can reproduce the observed hydraulic heads in the different boreholes, the Nash-Sutcliffe Efficiency (NSE) was calculated and provided a satisfying value of 0.99 for the observation well P2.2.

The results for P2.2 are plotted in Figure 7. The retardation coefficient estimated during the inversion varies between 20 and 150 m over the study period (Figure 7, red dots) suggesting the transient nature of the streambed conductance. Figure 7 also shows the minimal value of the *SSE* reached during each estimation of a (yellow triangles).

4.3. Interpretation of the Field Data Analysis

The time line of the study period has been subdivided in five periods. These subperiods are characterized by different states and dynamics of the gradient between the Rhône River and the riparian water table.

Periods (1) (see Figures 6 and 7): These annual low water seasons (approximatively between November and April) are characterized by a Rhône River stage lower than the riparian water table. Due to the

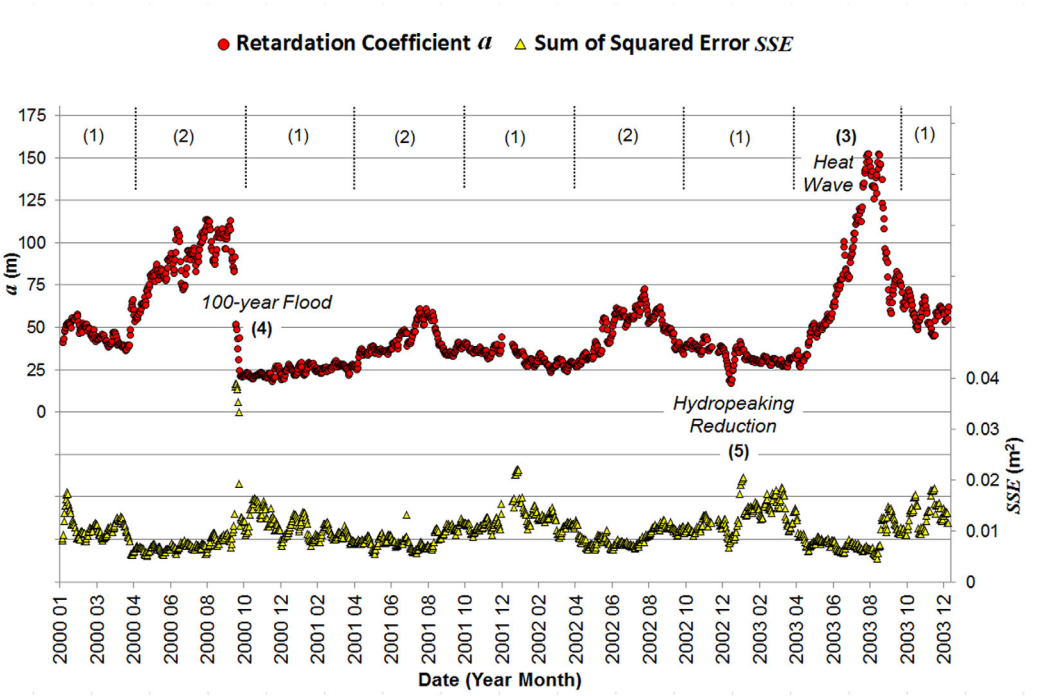

Figure 7. Plot of the estimated value of the retardation coefficient, *a*, for the observation well P2.2 (red dots). Value of the residual sum of squares *SSE* between field and simulated hydraulic heads for each POW (yellow triangles). The highest value of *SSE* occurred when the retardation coefficient varies strongly (100 year flood). (1), (2), (3), (4), and (5) refers to the periods described in Figure 6.

hydroelectricity generation, the level of the Rhône River increases and decreases on a daily basis (especially during the week, period where energy demand is high) with an amplitude of about 1 m (see Figure 5). Within this period, no significant variations of the retardation coefficient is observed (variations of *a* around 10 m). This stability could be explained by periodic gradient inversion between the river and the groundwater: when the aquifer is drained by the river, fine sediments are partly washed away due to the upward seepage of groundwater. When the gradient is reversed (hydropeaking), fine sediments are deposited in the streambed, lowering the hydraulic conductivity and thus the streambed conductance. The alternation of erosion and deposition processes results in only minimal changes of the streambed conductance. This hypothesis can be supported by the rapid decrease of the retardation coefficient observed during the last weeks of December 2002 (Period (5), see Figure 6) when the hydropeaking is reduced significantly (see Figure 7, "Hydropeaking Reduction") at around 20% of its typical values during the investigated periods.

Periods (2) and period (3) (see Figures 6 and 7): During high water seasons (approximately between May and October), the parameter *a* increases. Within the entire study period, the value of *a* is approximatively 2–3 times higher during the high water periods than during the low water periods. In summer when the surface water level is constantly above the riparian water table, a unidirectional infiltration of the river tends to decrease the conductance of the streambed with the deposit of a large quantity of fine particles originating from overland flow generated by snowmelt. During the period (3), which corresponds also to high water season, a larger gradient (1 m to more than 2 m, Figure 6) and a stronger variation of *a*, compared to those in period (2), is observed. The reason of the exceptionally high stream stage during this period is the massive glacier melt caused by the heatwave of summer 2003. Between May 2003 and September 2003, the parameter *a* presents an increase of more than 200% (from 40 to 150 m over 4 months) with a slope of 1 md^{-1}. However, at the end of period (3), *a* undergoes a 60% decrease and reach a value of 60 m. This drop of *a* is concomitant with a decrease of the stream stage. The reduced gradient between the stream and the groundwater and its inversion may have caused an unclogging of the streambed (low water period, periods (1)).

Period (4) (see Figures 6 and 7): This period is marked by a 100 year flood event (Figure 6) occurring between 13 and 17 October 2000, with a climax on the 15 October. We can observe a drop of *a* (80% drop, see Figure 7), indicating a significant rise of the streambed conductance. The *SSE* (Figure 7) increases

significantly (250%) compared to its average value. As shown in section 3.2, the assumption of constant value of *a* within a POW can reduce the fit of simulated data with observed data when important and rapid changes of the streambed conductance occurs within the POW. It can be assumed that during the flood event high shear stress can mobilize the largest grains and stones (armor layer), protecting the finer grains trapped underneath, which are responsible for the low streambed hydraulic conductivity. The finer grains can be washed away and thus the streambed conductance increases [*Chin et al.*, 1994; *Schalchli*, 1992].

In order to assess to what extent the distance between a borehole and the river affects the results a correlation matrix of estimated *a* between the five observation wells was established (not shown). The correlation coefficients between the estimated *a* range from 0.88 to 0.98. Therefore the transience in streambed properties at this field site can be identified from different distances. All the above mentioned trends, obtained using observation well P2.2, were identify for the other observation wells.

5. Discussion

Several simplifying assumptions were made in the proposed methodology. For example, it is assumed that the distance *x* of the piezometer to the river does not change with a rising water table, which requires a rectangular shape of the river. This is a critical assumption and limits the applicability of the method to rivers with a rectangular shape, as the reduced distance between the river and the observation well will result in a decrease of *a*, even though there is no change in streambed conductance. For natural streams with an irregular bathymetry, caution is advised in the application of the proposed method.

Also, homogeneity is assumed for both the aquifer and streambed properties. This assumption is however not critical for the analysis. The estimated streambed conductance is representing the average hydraulic properties of the river reach in the vicinity of the borehole. Changes to the streambed structure due to erosion or deposition processes will affect the average hydraulic properties of the streambed, even if the streambed is heterogeneous. It is assumed that the river is fully penetrating and implies a one-dimensional water flux in a confined aquifer. However, influence of partially penetrating streambed can be reasonably lumped in the estimation of the retardation coefficient by substitution of an horizontal additional stretch of the main aquifer [*Hantush*, 1965].

It is also assumed that changes of the water table elevation are exclusively related to the transience in the river. This can pose a certain problem if additional hydraulic forcing is present, e.g., groundwater abstraction. To limit such effects, it is important that the observation well is close to the stream. In the field example discussed, however, transience of the streambed was identified for all observation wells (with a distance up to 44 m from the river).

As illustrated by the synthetic data analysis, we show that the choice of POW has a certain effect on the absolute values of *a*. The choice of a smaller POW size appears to be more suitable when sharp and sudden changes of the streambed conductance occur. On the other hand, the POW size should be large enough to include a significant amount of observations of stream stage variations and its related aquifer responses. However, for all POWs tested, we could clearly identify the imposed transience in the stream.

Finally, to employ the presented convolution approach, transience in the river is required. Therefore, the reliability of the estimation will be affected if the system is steady or lacking of transience in the stream. On one hand, streambed conductance transience can occur and yet not be detected because of the lack of floodwave response to analyze. On the other hand, calibration may result in wrong values of the retardation coefficient by fitting noise or measurement errors. This will be the case if insufficient transience is present in the stream. Therefore, the goodness of fit between observed and modeled data will provide a first indication on whether sufficient transience is present in the stream. Furthermore, the time series of data should have a sufficiently fine temporal resolution to capture these variations.

The interpretation of the results shows the relation between fluvial dynamics (climatic events) and streambed clogging and unclogging. The results obtained with the presented method confirm the influence of the magnitude of the gradient, its direction, and its dynamics (i.e., duration and intensity of the gradient variations) on the streambed conductance. Also, we observed that flood events (Period (4)) can cause an increase in the streambed conductance probably due to important alteration and erosion of the riverbed sedimentary structure.

6. Conclusions

The hydraulic properties of the streambed control surface water-groundwater interactions. However, hydraulic properties are hard to measure, and detecting transience is even harder. Nevertheless, numerous field studies documented important changes of hydraulic properties, typically related to erosion and sedimentation processes. The method we propose aims at rapidly identifying transience in streambed conductance. To apply the method, time series of river stage and water table data are required, as well as a certain transience in the river. The rivers need to have a rectangular shape. If these conditions are given, the approach has significant advantages compared to directly measuring hydraulic properties in the streambed. It is very simple in terms of field instrumentation and workload. Moreover, the estimation can be done on very large or fast flowing rivers where direct measurements of the streambed hydraulic properties are virtually impossible. However, given the simplifying assumptions our approach is based on, it is important to note that if no transience is detected, this is no conclusive proof that streambed properties are constant.

The method has been successfully employed to a field case, and a clear transience in the streambed conductance was identified. This has important implications on any quantitative approach aimed at understanding the dynamics between surface and groundwater in this region. Above all, this transience should be considered in future modeling approaches.

Acknowledgments
This study was funded by the project Third Rhône River Restoration (website: http://www.rhone3.ch) and the Swiss Confederation. The authors wish to thank Ben O'Connor, the two anonymous reviewers and the associate editor for their helpful comments and suggestions. The data used in this paper were also generously provided by the Third Rhône Restoration Project. The data and the numerical results used and produced in this paper are available upon request to the corresponding author Guillaume Gianni at guillaume.gianni@unine.ch.

References

Besson, O., J. Rouiller, W. Frei, and H. Masson (1991), Campagne de sismique-reflexion dans la vallée du Rhône (entre Sion et Martigny, Suisse), *Bull. Murithienne*, *109*, 45–63.
Calver, A. (2001), Riverbed permeabilities: Information from pooled data, *Ground Water*, *39*(4), 546–553.
Carslaw, H. S., and J. C. Jaeger (1959), *Conduction of Heat in Solids*, 2nd ed., Oxford at the Clarendon Press, London, U. K.
Chin, C. O., B. W. Melville, and A. J. Raudkivi (1994), Streambed Armoring, *J. Hydraul. Eng.*, *120*(8), 899–918.
Coleman, J. M. (1969), Brahmaputra river: Channel processes and sedimentation, *Sediment Geol.*, *3*(2–3), 129–239.
Du, X. Q., Z. J. Wang, and X. Y. Ye (2013), Potential Clogging and Dissolution Effects During Artificial Recharge of Groundwater Using Potable Water, *Water Resour. Manage.*, *27*(10), 3573–3583.
Fette, M., R. Kipfer, C. J. Schubert, E. Hoehn, and B. Wehrli (2005), Assessing river-groundwater exchange in the regulated Rhone River (Switzerland) using stable isotopes and geochemical tracers, *Appl. Geochem.*, *20*(4), 701–712.
Genereux, D. P., S. Leahy, H. Mitasova, C. D. Kennedy, and D. R. Corbett (2008), Spatial and temporal variability of streambed hydraulic conductivity in West Bear Creek, North Carolina, USA, *J. Hydrol.*, *358*(3-4), 332–353.
Ha, K., D. C. Koh, B. W. Yum, and K. K. Lee (2007), Estimation of layered aquifer diffusivity and river resistance using flood wave response model, *J. Hydrol.*, *337*(3-4), 284–293.
Hall, F. R., and A. F. Moench (1972), Application of convolution equation to stream-aquifer relationships, *Water Resour. Res.*, *8*(2), 487–493.
Hantush, M. S. (1965), Wells near streams with semipervious beds, *J. Geophys. Res.*, *70*(12), 2829–2838.
Hatch, C. E., A. T. Fisher, C. R. Ruehl, and G. Stemler (2010), Spatial and temporal variations in streambed hydraulic conductivity quantified with time-series thermal methods, *J. Hydrol.*, *389*(3–4), 276–288.
Hiscock, K. M., and T. Grischek (2002), Attenuation of groundwater pollution by bank filtration, *J. Hydrol.*, *266*(3-4), 139–144.
HydroGeoSphere (2013), *User Manual*, Anquanty Inc., Waterloo, Ontario, Canada.
Irvine, D. J., P. Brunner, H. J. H. Franssen, and C. T. Simmons (2012), Heterogeneous or homogeneous? Implications of simplifying heterogeneous streambeds in models of losing streams, *J. Hydrol.*, *424*, 16–23.
Jha, M. K., and A. Singh (2014), Application of genetic algorithm technique to inverse modeling of tide-aquifer interaction, *Environ. Earth Sci.*, *71*(8), 3655–3672.
Jha, M. K., K. Jayalekshmi, D. Machiwal, Y. Kamii, and K. Chikamori (2004), Determination of hydraulic parameters of an unconfined alluvial aquifer by the floodwave-response technique, *Hydrogeol. J.*, *12*(6), 628–642.
Jha, M. K., D. Namgial, Y. Kamii, and S. Peiffer (2008), Hydraulic parameters of coastal aquifer systems by direct methods and an extended tide: Aquifer interaction technique, *Water Resour. Manage.*, *22*(12), 1899–1923.
Kalbus, E., C. Schmidt, J. W. Molson, F. Reinstorf, and M. Schirmer (2009), Influence of aquifer and streambed heterogeneity on the distribution of groundwater discharge, *Hydrol. Earth Syst. Sci.*, *13*(1), 69–77.
Kollet, S. J., and V. A. Zlotnik (2007), Evaluation of the streambed leakage concept in analytical models using data from three pumping tests, *Hydrogeol. J.*, *15*(6), 1051–1062.
Kurth, A. M., and M. Schirmer (2014), Thirty years of river restoration in Switzerland: implemented measures and lessons learned, *Environ. Earth Sci.*, *72*(6), 2065–2079.
Landon, M. K., D. L. Rus, and F. E. Harvey (2001), Comparison of instream methods for measuring hydraulic conductivity in sandy streambeds, *Ground Water*, *39*(6), 870–885.
Lee, B. J., J. H. Lee, H. Yoon, and E. Lee (2015), Hydraulic experiments for determination of in-situ hydraulic conductivity of submerged sediments, *Sci. Rep.*, *5*, 7917.
Levy, J., M. D. Birck, S. Mutiti, K. C. Kilroy, B. Windeler, O. Idris, and L. N. Allen (2011), The impact of storm events on a riverbed system and its hydraulic conductivity at a site of induced infiltration, *J. Environ. Manage.*, *92*(8), 1960–1971.
MATLAB (2014), *8.3.0.532 (R2014a)*, The MathWorks Inc., Natick, Mass.
Mutiti, S., and J. Levy (2010), Using temperature modeling to investigate the temporal variability of riverbed hydraulic conductivity during storm events, *J. Hydrol.*, *388*(3-4), 321–334.
Reynolds, R. J. (1987), Diffusivity of a glacial-outwash aquifer by the floodwave-response technique, *Ground Water*, *25*(3), 290–299.
Rosenberry, D. O. (2008), A seepage meter designed for use in flowing water, *J. Hydrol.*, *359*(1–2), 118–130.
Rosenberry, D. O., and J. Pitlick (2009), Effects of sediment transport and seepage direction on hydraulic properties at the sediment-water interface of hyporheic settings, *J. Hydrol.*, *373*(3–4), 377–391.

Schalchli, U. (1992), The clogging of coarse gravel river beds by fine sediment, *Hydrobiologia*, *235*, 189–197.
Shanafield, M., R. G. Niswonger, D. E. Prudic, G. Pohll, R. Susfalk, and S. Panday (2014), A method for estimating spatially variable seepage and hydraulic conductivity in channels with very mild slopes, *Hydrol. Processes*, *28*(1), 51–61.
Simpson, S. C., and T. Meixner (2012), Modeling effects of floods on streambed hydraulic conductivity and groundwater-surface water interactions, *Water Resour. Res.*, *48*, W02515, doi:10.1029/2011WR011022.
Smith, J. W. N., and D. N. Lerner (2008), Geomorphologic control on pollutant retardation at the groundwater-surface water interface, *Hydrol. Processes*, *22*(24), 4679–4694.
Sophocleous, M. (2002), Interactions between groundwater and surface water: the state of the science, *Hydrogeol. J.*, *10*(1), 52–67.
Wang, T. Z., Y. K. Li, M. C. Liang, P. L. Yang, and Z. H. Bai (2014), Biofilms on the surface of gravels and aquatic plants in rivers and lakes with reusing reclaimed water, *Environ. Earth Sci.*, *72*(3), 743–755.
Winter, T. C., J. W. Harwey, O. L. Franke, and W. M. Alley (1998), Ground water and surface water: A single resource, *U.S. Geol. Surv. Circ.*, *1139*, 79 pp.
Woessner, W. W., and K. E. Sullivan (1984), Results of seepage meter and mini-piezometer Study, Lake Mead, Nevada, *Ground Water*, *22*(5), 561–568.
Wu, G., L. C. Shu, X. Lu, X. Chen, X. Zhang, E. K. Appiah-Adjei, and J. Zhu, (2015), Variations of streambed vertical hydraulic conductivity before and after a flood season, *Hydrogeol. J.*, *23*(7), 1603–1615.